

IMPEDANCES OF THE ELECTROLYTICAL RECTIFIER

by J. W. A. SCHOLTE and W. Ch. van GEEL

621.314.64.011.21

Summary

The system aluminium | aluminium oxide | electrolyte is a rectifier. The conductivity of the layers out of which the oxide is composed changes with the externally applied electrical potential difference. In this article a method is described, to derive from the frequency dependence of the impedance an electrical equivalent circuit of the oxide layer, consisting of a number of condensers with resistances in parallel. For the various states in which the oxide layer can be brought by means of D.C. tensions of different directions and values, diagrams are given, in which the specific resistance is shown as a function of the position in the oxide layer. All diagrams show a layer with a high resistance in addition to a layer in which the resistance decreases strongly. With electrical fields in the direction of good conductivity whereby no permanent change of the oxide appears, only the resistance of the high-resistance part varies with the external tension. In stronger electrical fields, causing a permanent change of the oxide layer, a mutual shifting of the more and less conducting layers appears. The electrical equivalent circuit is a starting point for a discussion on the material structure of the oxide layer. The conclusion is that both at the boundary with the aluminium as at the boundary with the electrolyte, the composition of the oxide shows a deviation from simple stoichiometric ratio and is a semiconductor. It is assumed that rectification occurs by means of the contact between *p*-type and *n*-type semiconducting layers.

Résumé

Le système aluminium | oxyde d'aluminium | électrolyte est un redresseur. Sous l'influence d'un champ électrique extérieur la conductibilité des couches dont se compose l'oxyde peut changer. Dans cet article, nous décrivons une méthode qui permet de déduire, des variations de son impédance en fonction de la fréquence, un schéma équivalent pour la couche d'oxyde. Ce schéma apparaît comme un certain nombre de condensateurs montés en série avec des résistances en parallèle. Les schémas équivalents ont permis d'établir des diagrammes, qui donnent la résistance spécifique aux différents endroits de la couche d'oxyde; ces diagrammes se rapportent aux différents états dans lesquels on peut mettre la couche d'oxyde en lui appliquant des tensions continues de sens et d'intensité différents. Ces diagrammes montrent tous qu'il existe une couche très mauvaise conductrice suivie d'une couche intermédiaire dans laquelle la résistance diminue beaucoup, suivie à nouveau par une couche bonne conductrice. Lorsque le champ électrique ne provoque pas de modification permanente dans la couche d'oxyde, la résistance de la partie mauvaise conductrice varie avec la tension appliquée. Lorsque le champ électrique est assez intense pour provoquer un changement permanent dans la structure de la couche d'oxyde, les couches plus ou moins conductrices se déplacent les unes par rapport aux autres. Le schéma équivalent est le point de départ d'une discussion sur la structure de la couche. On conclut qu'à la limite Al_2O_3 -Al, de même qu'à la limite Al_2O_3 -électrolyte, la couche n'a pas la composition stœchiométrique mais contient des ions en excès, qui rendent ces pellicules

semi-conductrices. Le redressement provient du fait que les deux pellicules semi-conductrices ont des porteurs de charges de signes différents (semi-conducteur par électrons, et trous).

Zusammenfassung

Das Kombinationssystem Aluminium | Aluminiumoxyd | Elektrolyt stellt einen Gleichrichter da. Die elektrische Leitfähigkeit der Schichten aus welchen das Oxyd aufgebaut ist, ändert sich mit der außen angelegten elektrischen Spannung. In dieser Abhandlung wird eine Methode beschrieben mittels welche aus der Frequenzabhängigkeit des Scheinwiderstandes ein elektrisches Ersatzbild der Oxydschicht, bestehend aus einer Anzahl Kondensatoren mit parallel geschalteten Widerständen, gewonnen werden kann. Für die verschiedenen Zustände, in welche die Oxydschicht durch Gleichspannungen verschiedener Richtung und verschiedener Größe versetzt werden kann, werden aus diesem Ersatzbild Kennlinien abgeleitet, in denen der spezifische Widerstand als Funktion der Entfernung von den Elektroden wiedergegeben ist. Diese Kennlinien zeigen alle eine Schicht mit hohem Widerstand sowie eine solche mit stark abnehmendem Widerstand. Unter der Einwirkung elektrischer Felder, bei denen keine bleibende Veränderung der Oxydschicht auftritt, ändert sich nur der Widerstandswert des Teiles mit dem höherem Widerstand. Durch starke elektrische Felder, die eine bleibende Veränderung der Oxydschicht zur Folge haben, tritt eine gegenseitige Verschiebung der mehr und weniger leitenden Schichten auf. Das elektrische Ersatzbild bildet den Ausgangspunkt für eine Diskussion über den strukturellen Aufbau der genannten Schicht. Es wird festgestellt, daß sowohl an der Aluminiumseite als auch an der Elektrolytseite das Aluminiumoxyd eine stöchiometrische Abweichung zeigt und einen Halbleiter darstellt. Die Gleichrichtung kommt durch den Kontakt zwischen Defekt- und Überschußhalbleiter zustande.

1. Introduction

The oxide layer formed on aluminium by anodical oxidation in a solution of boric acid and sodium borate, has rectifying properties. The highest resistance appears when the aluminium is positive. With the asymmetry in the electrical properties there corresponds an asymmetry in the structure of the oxide layer. The oxide is composed of layers that differ according to whether they are situated at the aluminium side or at the electrolyte side.

From impedance measurements, over a wide range of frequencies, on oxide layers of different thicknesses, we earlier found ¹⁾ that the dielectric losses are inversely proportional to the thickness of the layer. Measurements of the capacity at frequencies so high that no dependence of the frequency appeared showed the relation $1/C = aV + \beta$ (C = capacity, V = forming voltage, a and β are constants). With a constant dielectric constant, the thickness d of the layer corresponds with $d = a'V + \beta'$. These facts can be accounted for by the conception that the oxide layer consists of a layer of constant thickness and with rather high parallel conductivity, and a layer with very low specific conductivity and of a thickness proportional to the forming voltage. From measurements of

the ballistic capacity¹⁾ it appeared that there existed a gradual transition between the layers of high resistance and the layers with low resistance. The complete oxide layer can be described by means of an electrical equivalent circuit consisting of a number of condensers in series, each with a resistor in parallel.

In this article a method will be given to determine from A.C. impedance measurements, the different resistances and capacities out of which the electrical equivalent circuit is composed. By interpreting each capacity with the resistance in parallel as the electrical equivalent of one thin layer of oxide, thin enough to be considered as homogeneous, diagrams can be drawn giving the distribution of the specific resistance over the thickness of the oxide layer.

Such an analysis has been given for Cu_2O rectifiers by Pfozter²⁾ and by Rose³⁾. Both authors, however, introduce certain approximations to get results. Pfozter supposes that the specific resistance can depend on the distance to the electrode only according to certain (theoretical) formulae. He calculates the impedances that arrive in those cases as a function of the frequency. By comparing them with the impedances measured the specific resistance of the various layers can be calculated. Rose neglects the layers having both ohmic and capacitive impedance. He assumes there is a boundary somewhere between the electrodes separating the layers into only ohmic and only capacitive ones.

The A.C. impedance is measured also with D.C. bias. In the blocking direction the D.C. voltage was equal to the forming voltage, in the transmission direction it was taken small enough as to cause no permanent change in the oxide (current $0.5-50 \mu\text{A}/\text{cm}^2$).

In the frequency range $12.5-20,000$ c/s the impedance was measured by means of an A.C. bridge. The A.C. measuring tension was so small that it was uninfluenced by the non-linearity of the current-voltage characteristic.

In section 2 we describe the measuring arrangement used. Section 3 concerns the development of a method to calculate the elements of the equivalent scheme from the measured impedances. In sections 4 and 5 the influence of the bias voltage is investigated. The effect of a D.C. voltage in the blocking direction appears to be small. By a tension in the direction of good conductivity, in the whole part of the oxide layer where the specific resistance is very high, the resistivity decreases at a uniform rate. The layers with relatively low specific resistances do not change until a considerable D.C. current increase. In section 6, some attention is given to the influence of thermal treatment on the composition of the oxide layer and also the influence of the pre-treatment (cleansing) of the aluminium. Finally, in section 7, an interpretation of the observed phenomena by means of the theory of semiconductors is given.

2. Measuring arrangement

The system aluminium | aluminium oxide | electrolyte the impedance of which is to be determined, is placed in the branch AC of a Wheatstone A.C. bridge (fig. 1). To neutralize parasitic capacities towards earth the bridge is provided with an auxiliary bridge according to Wagner. By means of this bridge, the potential of B is equalized to earth potential. The auxiliary bridge is adjusted by means of a resistance R_w and a capacity C_w .

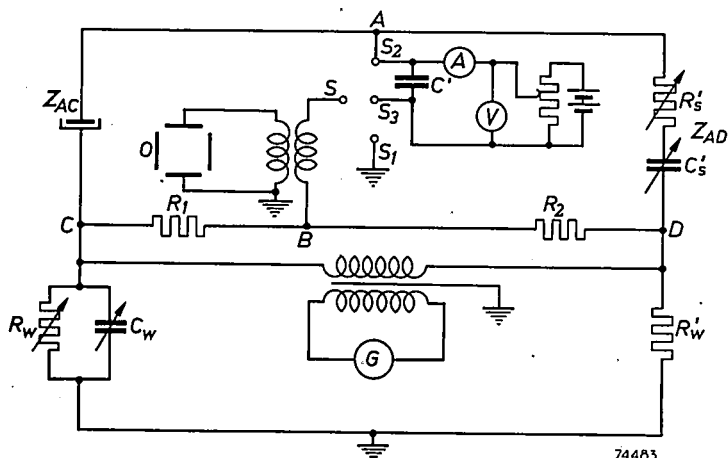


Fig. 1. A. C. Wheatstone bridge. The A. C. tension is to be superimposed on a D.C. tension.

The switch S is then in position S_1 . In position S_2 the impedance Z_{AC} is measured without any bias voltage on it. In position S_3 , on Z_{AC} is a bias voltage that can be regulated within wide limits. The condenser C' of large capacity ($120 \mu\text{F}$) forms the connection between A and S for the alternating current used for the measurements. The measuring tension is supplied by an audio-frequency generator G , giving frequencies up to 100,000 c/s. In the middle branch of the bridge there is a cathode-ray oscillograph O which is used as an indicator. The A.C. tension between A and B which must be regulated to zero, is amplified by a transformer and then connected with the vertical deflection plates of the oscillograph. The horizontal plates are connected with the synchronized time-base. If the current-tension characteristic is linear in the range covered by the measuring signal, a slight deviation of the right adjustment of the bridge branches is shown on the oscillograph as a pure sine-shaped image, having the same frequency as the tension supplied by the generator. This is an easy criterion that the right differential resistance is being measured.

3. Method of analyzing the measuring results

When the indicator in the branch AB of the bridge of fig. 1 shows no current, the impedances obey the relation

$$Z_{AC} : Z_{AD} = R_1 : R_2.$$

The impedance of the system aluminium | aluminium oxide | electrolyte in the branch AC is equivalent to an arrangement in series of R_s and C_s (fig. 2a) which one obtains by multiplying R'_s and dividing C'_s by the bridge ratio R_1/R_2 . C_s and R_s appear to depend on the frequency. With increasing frequency they decrease and approach a certain final value.

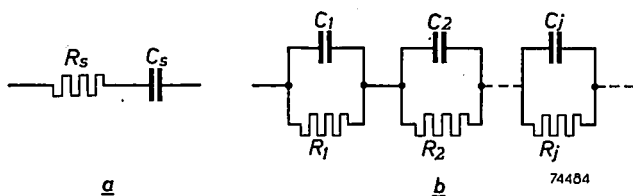


Fig. 2a. Arrangement in series of resistance and capacity, as measured on the bridge.
 2b. Electrical equivalent circuit of the aluminium-oxide layer, consisting of layers with different resistivities.

In a previous paper by the same authors¹⁾, it appeared that the Al oxide layer can be represented electrically by a circuit as shown in fig. 2b with frequency independent elements R_j , C_j ($j = 1, 2, \dots$). From the equivalence of the circuits of figs 2a and 2b follow the relations

$$R_s = \sum_j R_j F_j \quad (j = 1, 2, \dots), \quad (1)$$

$$\frac{1}{C_s} = \sum_j \frac{1}{C_j} G_j \quad (j = 1, 2, \dots), \quad (2)$$

where

$$F_j = \frac{1}{1 + \omega^2 R_j^2 C_j^2}, \quad G_j = \frac{\omega^2 R_j^2 C_j^2}{1 + \omega^2 R_j^2 C_j^2},$$

with $\omega = 2\pi f$ ($f =$ frequency).

It is possible to deduce from R_s and C_s (measured on the bridge as functions of ω) the values R_j and C_j ($j = 1, 2, \dots$).

Fig. 3 shows a logarithmic plot of

$$F = \frac{1}{1 + \omega^2 R^2 C^2} \quad \text{and} \quad G = \frac{\omega^2 R^2 C^2}{1 + \omega^2 R^2 C^2}$$

as functions of ωRC . For very small values of ω , F is about 1. For very

large values of ω it is about 0. It changes from 0.99 to 0.01 in the interval $0.1 < RC < 10$. In the same interval G changes from 0.01 to 0.99.

This means that in the summations (1) and (2), the functions F_j and G_j containing a product $R_j C_j$ greater than $10/\omega_1$, and the functions with a product $R_j C_j$ smaller than $0.1/\omega_2$ give a contribution that is either very small or independent of ω . For the frequency dependence of R_s and C_s between ω_1 and ω_2 ($\omega_1 < \omega_2$), only those functions F_j and G_j play a part that have a product $R_j C_j$ within the interval $0.1/\omega_2$ to $10/\omega_1$. We divide the circuit elements according to their value of the product $R_j C_j$.

(1) Elements with $\omega R_j C_j < 0.1$ for all measuring frequencies. Here the contribution to R_s equals R_j and the contribution to $1/C_s$ is very small. These elements behave like resistances throughout the whole range of frequencies investigated.

(2) Elements with $\omega R_j C_j > 10$ for all frequencies. The contribution to R_s is very small and the contribution to $1/C_s$ is about $1/C_j$. These elements behave like condensers.

(3) The interval between ($0.1 < \omega R_j C_j < 10$) has both ohmic and capacitive impedance. The elements give a contribution both to R_s and to $1/C_s$. The frequency dependence is shown in figs 3a and 3b.

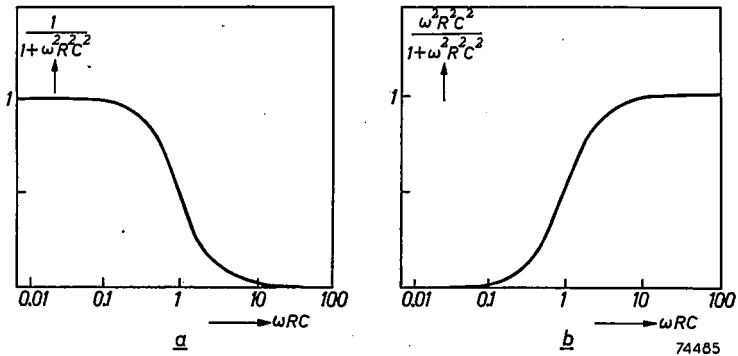


Fig. 3a. $\frac{1}{1 + \omega^2 R^2 C^2} = F$ as a function of ωRC .

3b. $\frac{\omega^2 R^2 C^2}{1 + \omega^2 R^2 C^2} = G$ as a function of ωRC .

The measuring frequencies covered a range from 12.5 to 20,000 c/s. So ω varied from 10^2 to 10^5 sec⁻¹. To the first group belong all elements with $R_j C_j < 10^{-6}$ sec, to the second group all elements with $R_j C_j > 10^{-1}$ sec. It is useful to write the summations (1) and (2) as follows

$$R_s = R_0 + \sum_j R_j F_j \quad (j = 1, 2, \dots), \quad (3)$$

$$\frac{1}{C_s} = \frac{1}{C_0} + \sum_j \frac{1}{C_j} G_j \quad (j = 1, 2, \dots). \quad (4)$$

In these equations, the products $R_j C_j$ under the summation sign are limited to the range 10^{-1} - 10^{-6} sec. R_0 is the sum of the resistances given above in group (1), $1/C_0$ is the sum of the reciprocal capacities of the second group.

R_s is linearly composed of the quantities F_j . By representing both R_s and a set of functions F_j in a diagram as functions of the frequency (scale $\log \omega$, see fig. 4) it is possible to construct R_s as the sum of the functions F_j each multiplied by a suitable coefficient. For each function this coefficient is the corresponding quantity R_j . Suppose, the number of measuring frequencies is n . Then condition (3) represents n linear equations with, say, m unknowns. The unknowns are the quantities R_0 and R_j . If the R_j of all products $R_j C_j$ are found, also C_j is known. About the C in parallel with R_0 we only know that it is less than $10^{-6}/R_0$ sec, for the first group of the classification given above concerns products $R_j C_j$ of less than 10^{-6} sec.

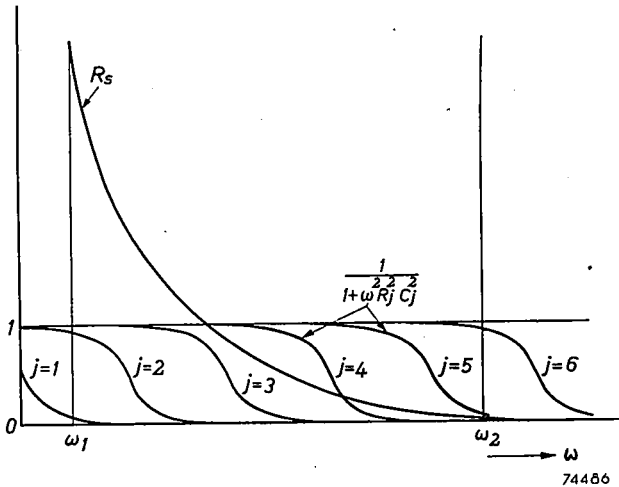


Fig. 4. R_s , measured between ω_1 and ω_2 is a linear superposition of a set of functions $\frac{1}{1 + \omega^2 R^2 C^2}$ (scale $\log \omega$).

There is, however, a further condition, namely $\frac{1}{C_s} = \sum_j \frac{1}{C_j} G_j$. Hence it follows, that the composition of $1/C_s$ as the sum of a series of functions G_j each multiplied by the coefficient $1/C_j$ must give the same C_j and R_j belonging to a given product $R_j C_j$ as did the analysis of the summation R_s . It appears that it is always possible to find a set of values R_j and C_j ,

satisfying both conditions (3) and (4) *). From the analysis of $1/C_s$ also follows the value of $1/C_0$. From the R in parallel with it we only know that $R > 10^{-1}/C_0$.

Summarizing, the following has been accomplished. In an interval, determined by the measuring frequencies, we chose a set of values $R_j C_j$, for instance forming a geometric series. We thereupon multiply the functions F_j and G_j by quantities R_j and $1/C_j$ respectively, having such values that a summation over j of these products agrees with the measured R_s and $1/C_s$ as well as possible. The result is a circuit, according to fig. 2b, behaving electrically exactly like the system under examination.

If the dielectric constant has in the whole oxide layer the same value, the deduced equivalent circuit is the representation of a series of layers, each with a thickness

$$\delta_j = \frac{\varepsilon A}{4\pi C_j}$$

and a (differential) resistivity

$$\rho_j = \frac{R_j A}{\delta_j} = \frac{4\pi}{\varepsilon} R_j C_j.$$

Here ε is the dielectric constant, given by an independent determination and A is the surface of the measured oxide layer. The result can be given graphically by a step function $\rho = \varphi(x)$, represented by a set of horizontal lines $\rho = \text{constant}$ (x is the distance to the outside of the oxide). The real function $\rho = \Phi(x)$ is represented by the bent curve agreeing as well as possible with the step function. See as an example fig. 5 of section 3.

Limitation of the possibilities and nature of the method of representation

We wish to make some remarks concerning the results that can be obtained with the method just described. If it was possible to measure with frequencies from 0 to ∞ , a complete electrical equivalent schema could be given. Our measuring range, however, was between 12.5 and 20,000 c/s.

*) By giving the real part of the impedance as a function of ω , the imaginary part is determined also at each frequency and vice versa. The complete impedance is a univalent analytical function of $i\omega$. With the theory of complex functions it is to be deduced, that under conditions that are satisfied in this case, the following relations exist between the real part and the imaginary part of the impedance 4):

$$x(\omega_1) = \frac{2}{\pi} \int_0^{\infty} \frac{\omega y(\omega)}{\omega_1^2 - \omega^2} d\omega,$$

$$y(\omega_1) = -\frac{2\omega_1}{\pi} \int_0^{\infty} \frac{x(\omega)}{\omega_1^2 - \omega^2} d\omega.$$

In the integrals must be taken the principal values.

Only those values of R_j and C_j can be determined for which the product $R_j C_j$ lays within the interval 10^{-1} to 10^{-6} sec. From the parallel circuits with a product $R_j C_j > 10^{-1}$ sec only the total capacity can be determined. From the circuits with $R_j C_j < 10^{-6}$ sec only the total resistance can be determined. The latter, however, is very small and cannot be distinguished from the series resistance caused by the electrolyte. The specific resistance is proportional to the product $R_j C_j$ namely $\rho_j = 4\pi R_j C_j / \epsilon$. So the measurement only leads to the determination of the thickness of the parts of the aluminium oxide layers, having specific resistances within certain limits. For layers corresponding with parallel circuits with $R_j C_j$ greater than 10^{-1} sec, only the total thickness is known, without the corresponding values of the resistances. The range of the specific resistances that can be determined is between 10^7 and 10^{10} Ωcm . Measured without D.C. bias the greater part of the Al oxide layer has a specific resistance greater than 10^{10} Ωcm and cannot be inserted in a ρ - x diagram. A favourable circumstance is that by applying a D.C. voltage in the direction of good conductivity, the specific differential resistance decreases so that the quantities $\omega R_j C_j$ come within the interval 0.1-10 and a determination of R_j is possible for all parts of the layer.

The A.C. measurements have been made at a fixed point of the D.C. current-voltage characteristic. This characteristic is non-linear. Therefore the resistances R_s and also R_j are differential resistances.

The capacities measured by a small A.C. voltage superimposed on the bias voltage are also differential quantities and so are the capacities C_j . At the greatest bias field strength used in our measurements, namely 10^7 V/cm in the blocking direction, the capacities appear to be independent of the D.C. voltage. With bias voltages in the transmission direction the D.C. electrical field strengths are much smaller. We now suppose that also here the dielectric displacement will be proportional to the applied electrical field.

It is clear that the impedance measurements can give no information on the successive order of the parallel connections in the electrical equivalent circuit. Other experiments must be made to obtain information regarding the real position of the oxide layers with high and with low specific resistances.

Finally, some remarks on the interpretation of the electrical equivalent circuit. The electrical properties of many "homogeneous" oxides lead to an equivalent scheme like that of fig. 2b. For such materials at least part of the losses can be ascribed to relaxation processes other than those caused by differences in D.C. conductivities. For these oxides $\tan \delta$ will not depend on the thickness of the material. For the Al_2O_3 layers investigated here, however, we know that $\tan \delta$ depends on the thickness. They are

composed of more and less conducting layers. Of course a certain fraction of the parallel conductivity of our layers might be due to relaxation processes.

Measurements on oxide layers after different pre-treatments of the aluminium used, appear to cause important differences regarding the losses. This fact shows that the losses are localized in a part of the oxide layer itself and that slow electrolytical processes consisting of an exchange of ions between oxide and electrolyte do not play an essential part.

Elaboration of an example

We will now give an example of the analysis given before. For an Al oxide layer, formed up to 100 volts, (thickness about 10^{-6} cm) the impedance was measured at frequencies from 12.5 to 20,000 c/s. The impedances were measured while a bias voltage was being applied, causing a current in the transmission direction of $4 \mu\text{A}/\text{cm}^2$. As described before only products $R_j C_j$ between 10^{-1} and 10^{-6} sec are concerned in the analysis. For practical reasons we here chose 5 products $R_j C_j$ namely $10^{-2.25}$, $10^{-2.5}$, 10^{-3} , 10^{-4} and 10^{-5} sec. In table I the functions F_j are given for the chosen values of $R_j C_j$ and for a number of frequencies, corresponding to the frequencies of the measurements.

TABLE I
 F_j for different values of ω and of $R_j C_j$

$\frac{\omega}{2\pi} (\text{sec}^{-1}) \downarrow$ / $R_j C_j (\text{sec}) \rightarrow$	$10^{-2.25}$	$10^{-2.5}$	10^{-3}	10^{-4}	10^{-5}	$<10^{-6}$
12.5	0.836	0.942	0.994	1	1	1
25	0.563	0.803	0.974	1	1	1
50	0.243	0.504	0.910	0.999	1	1
100	0.0741	0.203	0.717	0.996	1	1
300	0.0088	0.0274	0.220	0.966	1	1
1000	0.0008	0.0025	0.025	0.717	0.996	1
3000	0.0001	0.0003	0.0028	0.220	0.966	1
10,000	0.0000	0.0000	0.0003	0.025	0.717	1
20,000	0.0000	0.0000	0.0000	0.006	0.388	1

Because $R_s = R_0 + \sum_j R_j F_j$ the values of F_j from table I are to be multiplied by such values R_j , that the sum equals the measured R_s . In the case of this example there arise 9 equations with 6 unknowns. It is not

difficult to find the values of the unknowns satisfying the given equations within the measuring accuracy.

The result of the solution is given in table II. The first column shows the measuring frequencies, the last column the measured values of R_s . The first row shows the products $R_j C_j$, the second row the values of R_j , resulting from the equations. In the columns 2 to 6 are given the products $R_j F_j$ and in column 7 the quantity R_0 . The sum over j of these products is given in column 8. In general the agreement between the measured and the calculated values is rather good. Next the same method is applied to the relation $1/C_s = 1/C_0 + \sum_j (G_j/C_j)$. Here each function $G_j/(R_j C_j)$ is to be multiplied by R_j , so that a summation over j should give the $1/C_s$ that is measured. The results obtained by this method are given in table III. As we had to find a set of values R_j , satisfying both equations (3) and (4), in tables II and III the same values of R_j have been tried. It appears that one can indeed find a set of values R_j , belonging to the chosen set of products $R_j C_j$, that satisfy the equations (3) and (4). R_0 equals the electrolyte resistance within the measuring accuracy. In the example discussed here, $1/C_0$ is zero. Thus there are no layers with specific resistances, exceeding $10^{11} \Omega \text{ cm}$.

The results are shown in table IV and fig. 5a. In table IV are shown the values of R_j and C_j belonging to each value of the product $R_j C_j$. A layer of aluminium oxide corresponds with each parallel arrangement of the

TABLE II

$R_j F_j$ (in Ω) for different values of ω , $R_j C_j$ and R_j

$R_j \cdot C_j$ (sec) →	$10^{-2.25}$	$10^{-2.5}$	10^{-3}	10^{-4}	10^{-5}	$<10^{-6}$	$R_s = R_0 + \sum_j R_j F_j$	
R_j (Ω) →	1440	1800	44	12	1.8	R_0 (Ω)	calcu- lated	meas- ured
$\frac{\omega}{2\pi}$ (sec ⁻¹)								
↓ 12.5	1200	1690	44	12	1.8	13.4	2960	2880
25	810	1450	43	12	1.8	13.4	2330	2300
50	350	906	40	12	1.8	13.4	1323	1257
100	107	364	31	12	1.8	13.4	529	488
300	12.8	49.3	9.7	11.6	1.8	13.4	98.6	102
1000	1.1	4.6	1.1	8.6	1.8	13.4	30.6	30.5
3000	0.1	0.5	0.1	2.6	1.7	13.4	18.4	18.1
10,000	0.0	0.0	0.0	0.3	1.3	13.4	15.0	15.0
20,000	0.0	0.0	0.0	0.1	0.7	13.4	14.2	14.2

electrical equivalent circuit of fig. 2*b*. The thickness and the specific differential resistance of each thin layer are given by $\delta_j = R_j A / 4\pi C_j$ and $\rho_j = (4\pi/\epsilon) R_j C_j$. For the dielectric constant the value $\epsilon = 8.2^5$) is taken. In fig. 5*a*, the specific resistance of a thin layer is put as the

TABLE III

G_j/C_j (in μF^{-1}) for different values of $\omega, R_j C_j$ and R_j

$R_j C_j$ (sec) →	$10^{-2.25}$	$10^{-2.5}$	10^{-3}	10^{-4}	10^{-5}	$>10^{-1}$	$\frac{1}{C_s} = \frac{1}{C_0} + \sum_j \frac{G_j}{C_j}$	
R_j (Ω) →	1440	1800	44	12	1.8	$\frac{1}{C_0}$	calculated	measured
$\downarrow \frac{\omega}{2\pi}$ (sec $^{-1}$)								
12.5	0.042	0.032	—	—	—	—	0.074	0.075
25	0.112	0.112	0.001	—	—	—	0.225	0.246
50	0.195	0.283	0.004	—	—	—	0.482	0.496
100	0.236	0.453	0.012	0.001	—	—	0.702	0.705
300	0.255	0.553	0.034	0.004	—	—	0.846	0.852
1000	0.257	0.568	0.043	0.034	0.001	—	0.903	0.927
3000	0.257	0.570	0.044	0.094	0.006	—	0.971	0.978
10,000	0.257	0.570	0.044	0.117	0.049	—	1.037	1.040
20,000	0.257	0.570	0.044	0.119	0.110	—	1.100	1.100

TABLE IV

Survey of the quantities R_j and C_j of the electrical equivalent circuit and the values δ_j and ρ_j derived from it (Al_2O_3 layer, forming voltage 100 V, surface 19 cm 2 , current in transmission direction 80 μA)

$R_j C_j$ (sec)	for $A = 19$ cm 2		per cm 2		δ_j (10^{-6} cm)	ρ_j (Ω cm)
	R_j (Ω)	$\frac{1}{C_j}$ (μF^{-1})	R_j (Ω)	$\frac{1}{C_j}$ (μF^{-1})		
$10^{-2.25}$	1440	0.256	27,400	4.89	3.54	$7.74 \cdot 10^9$
$10^{-2.5}$	1800	0.568	34,200	10.80	7.83	$4.37 \cdot 10^9$
10^{-3}	44	0.044	840	0.84	0.61	$1.38 \cdot 10^9$
10^{-4}	12	0.12	228	2.28	1.65	$1.38 \cdot 10^8$
10^{-5}	1.8	0.18	34	3.4	2.46	$1.38 \cdot 10^7$

ordinate, and the thickness of the thin layer having that resistance as the abscissa. The five parallel arrangements of $R_j C_j$ from tables II, III, and IV are drawn as five functions $\rho = \text{constant}$. It is obvious to represent the real relation by a continuous bending curve, matched as well as possible to the step-shaped curve. By choosing more, for instance 8 instead of 5 parallel arrangements, the result was a step function giving practically the same function $\rho = \Phi(x)$. The number of parallel circuits is determined only by practical considerations.

In fig. 5b the same result is shown, however, with the layers, having the highest resistivity in the middle. This represents the situation,

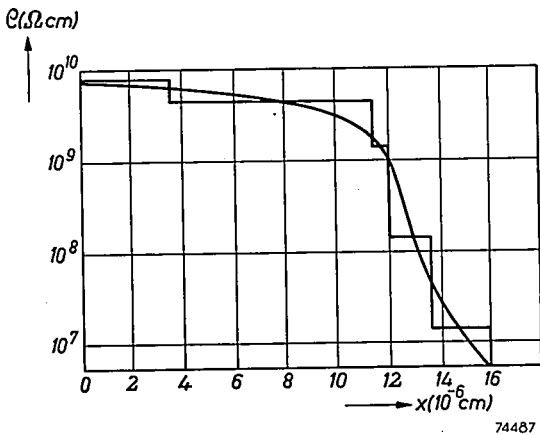
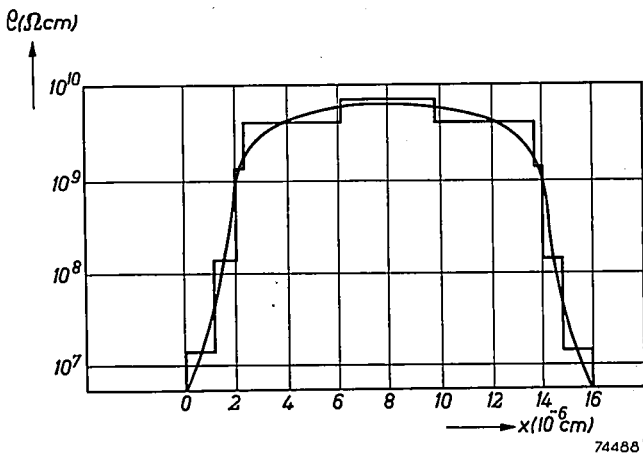


Fig. 5a. Differential resistivity as a function of the distance in the oxide layer. Forming tension is 100 V. Measured during 80 μ A D.C. current across 19 cm^2 surface. Order of sequence according to decreasing resistance.



5b. As 5a, but with the maximum resistance in the centre.

that both at the aluminium side and at the electrolyte side the specific resistance has been decreased. For instance by a deviation of the stoichiometry of the oxide.

4. Influence of bias voltage in the blocking direction

In the following, the results of the impedance measurements on aluminium oxide layers under different circumstances are described and developed by the method described previously.

TABLE V
Impedance per cm^2 of an Al_2O_3 layer formed up to 100 V

$\frac{\omega}{2\pi}$ (sec^{-1})	without bias voltage		with 100 V blocking voltage	
	R_s (Ω)	C_s (μF)	R_s (Ω)	C_s (μF)
25	3550	0.0660	3550	0.0662
50	2300	0.0648	2300	0.0650
100	1585	0.0635	1585	0.0636
300	765	0.0605	765	0.0606
1000	401	0.0577	401	0.0577
3000	297	0.0556	297	0.0556
6000	271	0.0541	271	0.0541
10,000	260	0.0527	260	0.0527
15,000	253	0.0512	253	0.0512
20,000	248	0.0501	248	0.0501

Table V shows the measured quantities R_s and C_s of an oxide layer made by oxidizing Al to 100 V in a solution of boric acid and sodium borate. In the columns 2 and 3, these are given for the case that no bias voltage was applied. This measurement concerns the A.C. impedance at the zero point of the i - V characteristic. The columns 4 and 5 of table V show R_s and C_s for the case that in the blocking direction a bias voltage equal to the forming voltage was present. Here the D.C. current was $0.3 \mu\text{A}/\text{cm}^2$. From 12.5 to 20,000 c/s the impedances with and without bias voltage did not differ. The condition of the layers in the oxide, having specific resistances within the interval open to the analysis is not influenced by a bias voltage in the blocking direction.

The result of the analysis of the measured impedance is shown in table VI and fig. 6. The specific resistance is shown in fig. 6 as a function of the

TABLE VI
Results derived from table V

RC (sec)	R (Ω)	$\frac{1}{C}$ (μF^{-1})	δ (10^{-6} cm)	ρ (Ωcm)
$> 10^{-1}$		14.6	10.7	$> 10^{11}$
10^{-2}	5700	0.57	0.4	$1.38 \cdot 10^{10}$
10^{-3}	1500	1.5	1.1	$1.38 \cdot 10^9$
10^{-4}	150	1.5	1.1	$1.38 \cdot 10^8$
10^{-5}	27	2.7	2.0	$1.38 \cdot 10^7$

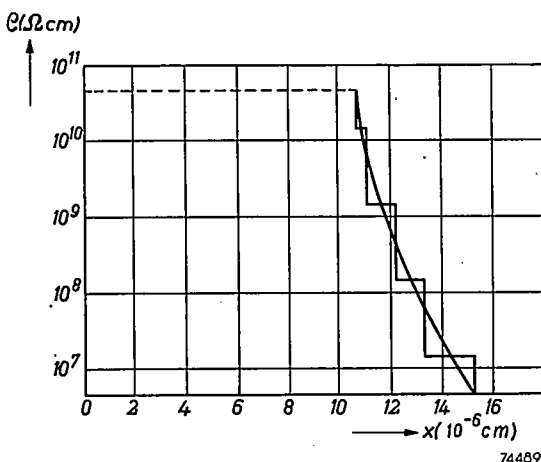


Fig. 6. $\rho = \varphi(x)$, both without any D.C. tension and with a D.C. tension equal to and in the same direction as the forming tension.

place in the oxide layer. The values of the differential resistances can be determined only for a small fraction of the total oxide thickness. The $\rho-x$ function is independent of a D.C. voltage and thus represents the specific resistance and not only the differential specific resistance. The specific resistance of the remaining part of the oxide layer is too high to be determined. This part expresses itself in the frequency range 12.5 to 20,000 c/s as pure capacities. The total thickness of this part is well known. Regarding its specific resistance we only know that it exceeds 10^{11} Ωcm .

5. Influence of direct current in the transmission direction

By making the Al electrode negative with respect to the electrolyte by a tension of 2 to 3 volts, a slowly increasing current will flow. After some minutes the current will have reached a value at which no further increase

will appear. It is only for small D.C. currents (less than 0.1 mA/cm^2) that the condition is sufficiently stationary for A.C. impedance measurements. By removal of the D.C. voltage two possibilities can arise:

(A). At small currents (up to 0.1 mA/cm^2) the oxide layer returns to its original state.

(B). At currents greater than 1 mA/cm^2 the oxide layer appears to have changed. We call this the deformed state.

The experiments may therefore be divided into two groups, according to the current densities mentioned above.

(A) Temporary changes of the oxide layer

Al was covered with oxide layers by anodic oxidation by forming voltages of 10, 30, 100 and 325 volts. The D.C. current flowing in the transmission direction through the oxide layer during observation was 10, 100 and $1000 \mu\text{A}$. The surface of the oxide layers was 24 cm^2 . The results of the impedance measurements were analyzed as described before. It appeared that under the applied transmission currents, the value of the differential resistances came always within the interval, in which its determination by means of the analysis was possible. The complete result is given in figs 7, 8, 9, and 10. These each show the relation between the specific differential resistance and the position in the layer, in the case of one thickness and with the value of the transmission current as parameter.

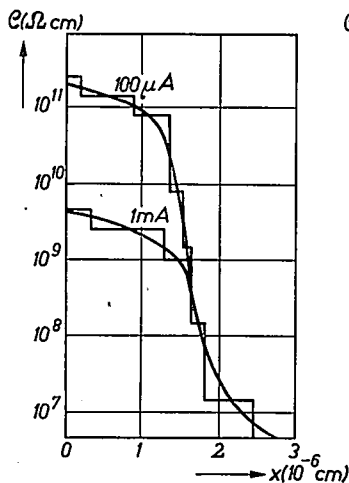


Fig. 7. $\rho = \varphi(x)$, during D.C. current in the transmission direction. Forming voltage 10 V. Direct current 100 and $1000 \mu\text{A}/24 \text{ cm}^2$.

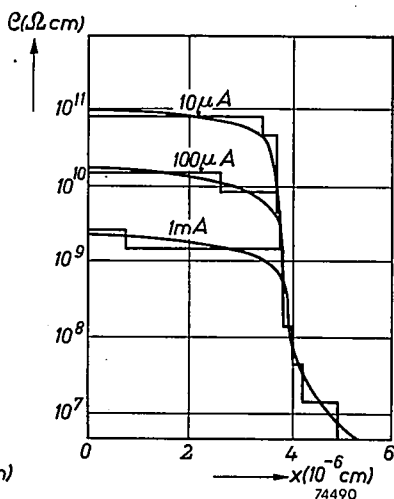


Fig. 8. $\rho = \varphi(x)$, during D.C. current in the transmission direction. Forming voltage 30 V. Direct current 10, 100 and $1000 \mu\text{A}/24 \text{ cm}^2$.

From this result one may conclude:

- (1) The differential resistance $\rho_{diff.} \equiv dV/di$ is nearly constant in the larger part of the oxide layer. In a small part it decreases to a small value.
- (2) At each thickness of the oxide layer, an increase of the D.C. current corresponds to a decrease of $\rho_{diff.}$ of the most insulating part of the layer. Generally, in the boundary range of the layer at the side where $\rho_{diff.}$ is less, no change is to be observed. As $\rho_{diff.}$ is here independent of the D.C. tension, it will equal the specific resistance itself. An increase of the current by a factor 10 corresponds to a decrease of the differential resistance of nearly a factor 10 in the most insulating part of the layer.
- (3) At equal currents in the transmission direction, thick oxide layers

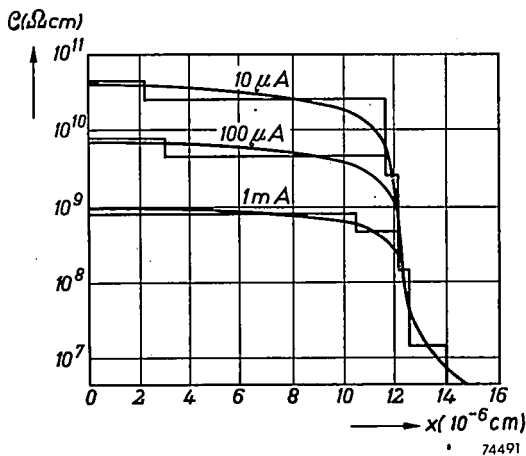


Fig. 9. $\rho = \varphi(x)$, during D.C. current in the transmission direction. Forming voltage 100 V. Direct current 10, 100 and 1000 $\mu\text{A}/24\text{ cm}^2$.

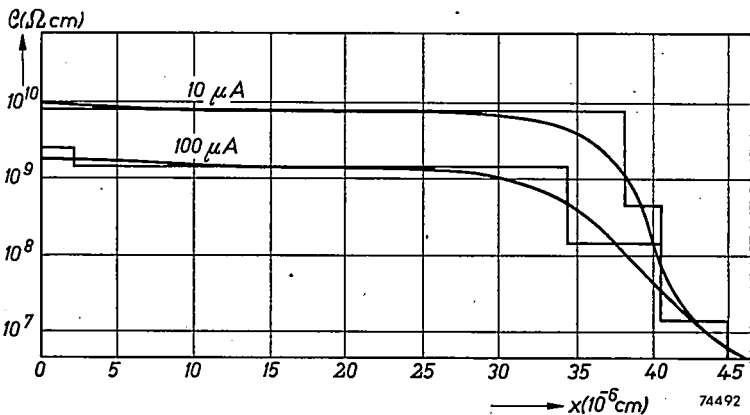


Fig. 10. $\rho = \varphi(x)$, during D.C. current in the transmission direction. Forming voltage 325 V. Direct current 10 and 100 $\mu\text{A}/24\text{ cm}^2$.

show lower ρ_{diff} values than thin layers. In thicker layers also the change of ρ_{diff} as a function of the position in the layer is smaller than in thinner layers. (4) By summation of ρ_{diff} over all layers of the oxide, one gets the total differential resistance. From the values of the D.C. voltage and current one gets the D.C. resistance. A conclusion to be drawn from the measurements is that the ratio of the total differential resistance to the D.C. resistance is in the order of 0.1. A check on the results given above would be a measurement of the D.C. characteristic in the transmission direction followed by a determination of dV/di . It is not possible, however, to check with sufficient accuracy that the slope dV/di in each point of the characteristic where an A.C. measurement has also been made, corresponds with the total differential resistance at that point.

Also while the D.C. current is flowing, two regions can be distinguished in the oxide layer. A region with nearly constant high resistance, decreasing under the influence of the D.C. current and a region, in which the resistance falls off sharply to low values. Apparently, the magnitude of the D.C. current exerts an influence on the resistance of the more insulating region.

A very large capacity with a very high resistance can be present in the equivalent circuit. This would mean a very thin layer with very high specific resistance. The existence of such a layer is rather difficult to check because at the measuring frequencies its contribution both to R_s and to $1/C_s$ is negligible.

(B) *Permanent changes of the oxide layer*

The second group of measurements concerns Al oxide layers that are deformed by means of a large current (for instance 5 mA/cm²) in the transmission direction. While this current is flowing the situation is so little stable that an impedance measurement is not possible. The measurements are made on an oxide layer, formed by the anodic oxidation of Al to 100 volts. Deformation took place for 2, 10 and 30 minutes successively. All deformations were followed by a partial recovery by applying voltages (5, 20, 100 V) in the reverse direction for 10 minutes. After all deformations and recoveries, impedance and ballistic-capacity measurements were carried out.

The ballistic capacities observed are shown in table VII and in fig. 11. The charging tension at each measurement was 5 volts. The capacities appear to increase when the deformation current is applied for a longer time. By means of voltages increasing in steps, the original capacity (0.061 $\mu\text{F}/\text{cm}^2$) is recoverable. That the deformation process is not merely a dissolving of the oxide layer may appear from the fact that with reforming to a rather low tension (5 volts, 20 volts) the capacity again approaches the capacity of the original layer.

TABLE VII

Ballistic capacity after deforming followed by partial recovery (forming voltage 100 V, surface of the plate 24 cm²)

deformed (in transmis- sion direction)	recovery (in blocking direction)		
	10 min, 5 V	10 min, 20 V	10 min, 100 V
100 mA, 2 min	0.069 $\mu\text{F}/\text{cm}^2$	0.061 $\mu\text{F}/\text{cm}^2$	0.061 $\mu\text{F}/\text{cm}^2$.
100 mA, 10 min	0.091	0.067	0.061
100 mA, 30 min	0.115	0.073	0.061

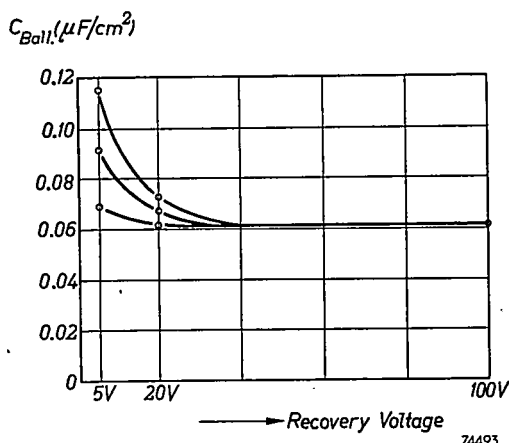
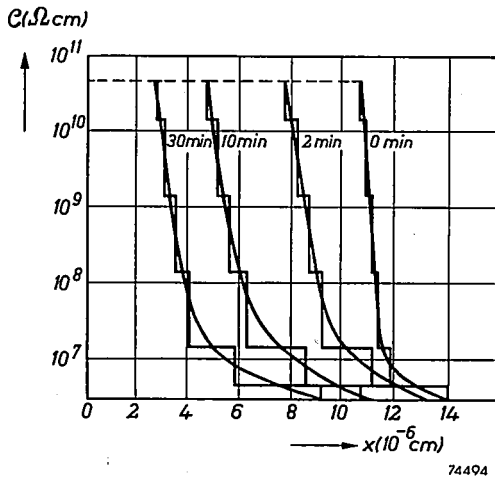


Fig. 11. Ballistic capacity, as a function of the recovery tension after previous deformation by 100 mA/24 cm². Upper curve: deformed for 30 minutes, central curve: deformed for 10 minutes, lower curve: deformed for 2 minutes.

The results of the bridge measurements are shown in figs 12 and 13. In these figures, the relation is given between the specific resistance and the distance to the boundary of the oxide layer. The diagrams were again made by means of the method described in section 3. Fig. 12 shows the dependence on the deformation time without any recovering having taken place.

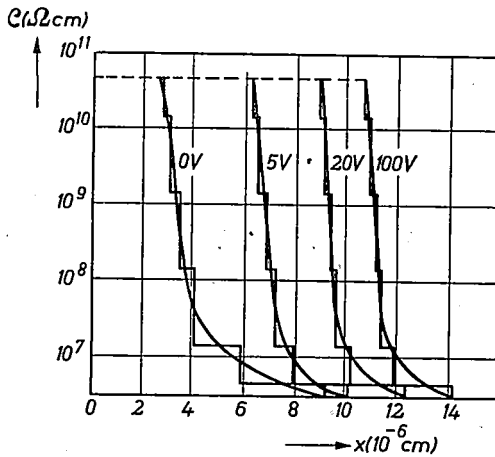
Fig. 13 shows the dependence on the recovery voltages. It appears that in contrast to the non-permanent deformation one can state that the boundary between the part with a high and a low resistance is shifted towards the high-resistance side. That this can be continued very much further is shown in the curve of fig. 12 in which the deformation current has flowed

for 30 minutes. The thickness of the insulating layer has decreased here to nearly one fourth of the original value. That deformation is not a dissolving of the oxide layer also appears from the recovery curves of fig. 13. After applying a tension of 5 V the thickness of the insulating part has doubled, after 20 V tension it is again 80% of the original value. For the smallest values of ρ , in the lower part of the figure, the curves will approach each other. The slope of the curves of fig. 13 is greater than the slope of the curves of fig. 12. The recovery seems to start from the layer with the highest resistance. This results in a greater slope of the curves representing the resistance as a function of the position in the oxide layer.



74494

Fig. 12. $\rho = \varphi(x)$, after a deformation of $100 \text{ mA}/24 \text{ cm}^2$ for 0, 2, 10 and 30 minutes. Forming voltage 100 V.



74495

Fig. 13. $\rho = \varphi(x)$, of the deformed oxide layer (deformed by $100 \text{ mA}/24 \text{ cm}^2$ for 30 minutes) after recovery by 0, 5, 20 and 100 V for 10 minutes. Forming voltage 100 V.

In fig. 14 the $\rho = \varphi(x)$ curve is given for an oxide layer formed to 100 V. Measurements have been made during the flow of 100 μA in the transmission direction. Fig. 14a applies to a layer that underwent no permanent deformation. Fig. 14b applies to a layer that was changed before the impedance measurements were made, by applying a deformation current of 5 mA/cm² for 30 minutes. In fig. 14b is shown the non-permanent effect combined with the permanent effect. In both cases the 100 μA current results in a decrease of the resistance of the less conducting

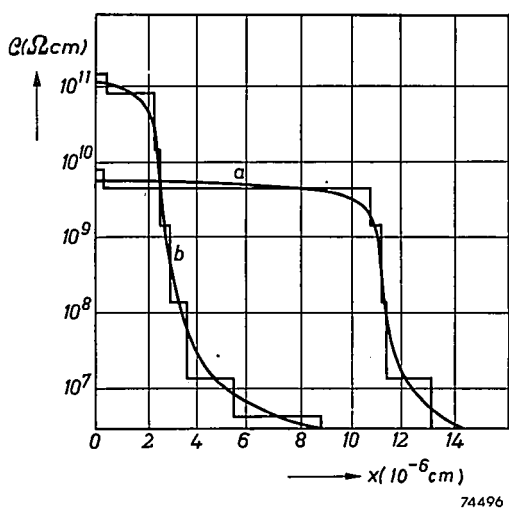


Fig. 14. $\rho = \varphi(x)$ during a transmission current of 100 $\mu\text{A}/24\ \text{cm}^2$. (a) in a non-deformed oxide layer, (b) in a deformed oxide layer.

part of the oxide layer, but in the layer deformed before, the resistance remains about 10 times as high as in the non-deformed layer. Here we can draw a parallel with the experiments of part (A) of this section. By a comparison of figs 7 to 10 we have seen that with the same current in the transmission direction, the specific resistance of the less conducting part of Al oxide layers is much higher when the layer is thinner. If the thickness of the less conducting part has been reduced by a deformation, the resistance of this part decreases less by a temporary deformation as for the case that this part had retained its original thickness.

6. Influence of a thermal treatment and of a pre-treatment of the aluminium

In an earlier paper¹⁾ we already showed that after heating in air for some hours at 450 $^{\circ}\text{C}$, the thickness of the relatively well conducting part of the oxide layer decreases by half its original value. An analysis

of its impedance before and after heating gives the same results. In fig. 15 the relation between the specific differential resistance and the position in the layer is shown for the same oxide layer, before and after the heating process.

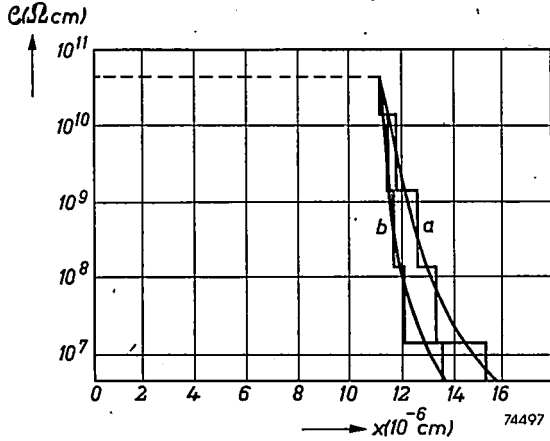


Fig. 15. Influence of an annealing process. (a) $\rho = \varphi(x)$, before annealing; (b) $\rho = \varphi(x)$, after annealing.

The surface of the Al was treated in two different ways. The first treatment consists only in a cleaning of the metal surface with alcohol. In the second process, a complete dissolving of the upper layer took place by alternate immersion in hot KOH and HNO₃, and afterwards in ammonia and citric acid. The difference is seen in fig. 16. When an oxide layer is

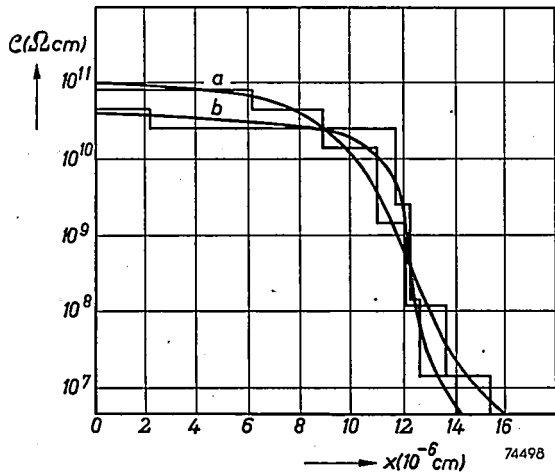


Fig. 16. Influence of the pre-treatment. (a) $\rho = \varphi(x)$, Al cleaned in successive baths of strong and weak bases and acids; (b) $\rho = \varphi(x)$, Al cleaned only superficially.

formed on aluminium cleaned according to the second method, the high-resistance part is thinner, the low-resistance part is thicker and the transition between these layers is much more gradual.

From the experiments described above, the example of section 3 (fig. 5) and the measurements under reverse current (fig. 6) have been made with aluminium treated according to method 2. All deformation experiments have been carried out with aluminium that has been treated according to method 1 (figs 7 to 14).

7. Survey and conclusion

In order to obtain further information, regarding the composition of the rectifying system aluminium | aluminium oxide | electrolyte, and the processes occurring during rectification, impedance measurements have been made on the system, while it was being brought by a constant direct current to a certain state of blocking or low resistance. The measuring results of the impedance are used in making diagrams, in which a distribution of the electrical conductivity over the thickness of the oxide layer is represented. All diagrams show a greater part in which the conductivity has a small nearly constant value, and a smaller part showing a considerable gradient in the conductivity, going from small to much higher values.

We distinguish between the experiments where the electrical field causes no permanent change in the oxide layer, and where changes occur.

In the first series of experiments, the electrical field strengths used are so small, that ionic conductivity can be excluded. The conduction is determined by the presence and the behaviour of free electrons and "holes". Most probably the occurrence of free electrons and holes is closely connected to deviations from simple stoichiometric ratio. According to Verwey⁶), the oxide formed by anodical oxidation consists of a face-centred lattice of oxygen ions, while the cations are distributed statistically over the available tetrahedral and octahedral interstices. It may be considered as a disordered cubic γ -structure⁷). Only a fraction of the interstices is occupied. If it is possible to add more aluminium atoms by occupation of more cation sites than corresponds to the stoichiometric composition, the valence electrons of this extra Al can go partly into the conduction band of the lattice and cause conduction by electrons. In the same way, a composition with less aluminium atoms than corresponds to the stoichiometric ratio would lead to the presence of "defect electrons" (holes in the valence band). The part of the layer having a small conductivity will contain very few free electrons and holes. The electrons and holes present in this region will, for the greater part, not be in equilibrium concentration, but will have come from neighbouring regions with greater concentrations, since the life time of free electrons and holes is not zero.

The diagrams, resulting from the impedance measurements give no information on the nature of the conductivity, neither on the sequence of the more and less conducting layers. The following points, however, enable a conclusion to be reached.

(1) Hartmann⁸⁾ describes a change in the conductivity of sintered α - Al_2O_3 . By reduction, the conductivity increases, by oxidation it decreases again. This is a proof that α - Al_2O_3 can be brought, chemically, into an *n*-type semiconducting state.

(2) For the case that the oxide would consist only of *n*-type Al oxide, there would exist a contact at the boundary with the Al metal, giving, according to the theories of Schottky and Mott⁹⁾ rectification in the wrong direction, namely blocking for Al negative.

(3) Van Geel¹⁰⁾ found in an examination of the rectification in combinations aluminium | aluminium oxide | semiconductor, only rectification for *p*-type semiconductors. This was explained by supposing the aluminium oxide to be *n*-type at the metal side followed by a blocking layer of stoichiometric oxide, and possibly by a layer of *p*-type oxide at the side of the semiconductor.

(4) By deformation by a strong electric field, the conductivity of the Al oxide increases strongly. There remains, however, a layer with high specific resistance (fig. 12). In an oxide layer formed to 100 V this layer decreases, after deformation over a period of 5 hours to 10% of its original thickness, but it never disappears completely. This indicates that even for a very strong deformation, the oxide layer will not change completely into a single-type semiconductor.

Though, strictly speaking, there is no direct proof for the occurrence of a *p*-type layer, the theory of the *p-n* contact in semiconductors¹¹⁾ will be applied. Suppose that in an Al oxide layer an *n*-type semiconductor and a *p*-type semiconductor are separated by a stoichiometric central layer without electronic charge carriers¹²⁾. By applying only a weak electrical field, no ionic displacement will appear. If the *n*-type side is negative with respect to the *p*-type side, both electrons and holes will drift towards the central layer. Since a recombination does not occur instantly, the number of the charge carriers in this layer increases and also its conductivity *). This representation is in agreement with experimental results for small currents in the forward direction. From figs 7, 8, 9, and 10 it is to be seen that the conductivity of the central layer is increased, the boundary layers remaining unchanged. An electrical field in the opposite direction will decrease the conductivity in the central layer. The experiments give no information about the magnitude of the effect since

*) Moreover a more detailed discussion shows that also a concentration gradient of charge carriers must be taken into account which gives rise to a concentration E.M.F. ¹¹⁾.

the resistance of the central layer with and without blocking voltage is too high to be determined. The boundary layers do not change.

The blocking direction is the direction in which the aluminium is positive. This shows as might have been expected, that the side of the aluminium oxide having excess Al and being an *n*-type semiconductor must be situated at the Al metal side and the Al oxide having a deficiency of Al at the electrolyte side.

The permanent change of the impedance and of the electrical equivalent circuit by greater currents in the transmission direction corresponds with a shifting of the boundaries between more and less conducting layers (fig. 12). The permanent change may proceed in the following way. Seen in the direction from aluminium towards electrolyte, the oxide layer consists of an *n*-type semiconductor gradually changing into stoichiometric oxide that is nearly an insulator and changes again gradually into a *p*-type semiconductor. If an electric tension is applied, the greatest field will be in the nearly insulating central part of the oxide. The ionic conductivity is an exponential function of the field strength¹³). Therefore, in the central part, the ionic current will form a much greater fraction of the total current than in the boundary layers where most of the current is carried by electrons. If an electric tension is applied in the deformation direction (aluminium negative), the result will be a removal of positive ions from the boundary layer between stoichiometric oxide and *p*-type semiconductor towards the boundary between stoichiometric oxide and *n*-type semiconductor or, possibly, a removal of negative ions in the blocking direction (see fig. 17). In the layers showing a deviation from stoichiometry, the current consists almost entirely of electrons or holes. We assume that the ionic lattice permits only a small deviation from the stoichiometric composition. The deformation tension then results in an ionic displacement,

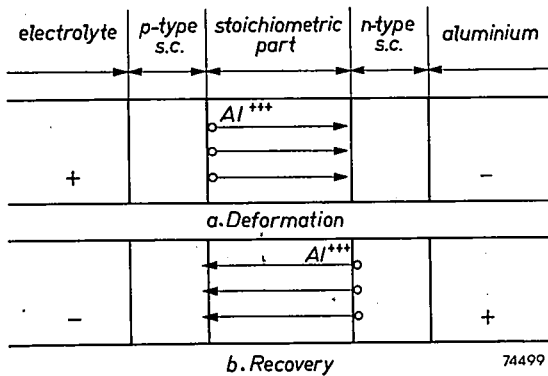


Fig. 17. Displacement of positive ions under influence of a strong electrical field in a system p-type semiconductor | stoichiometric layer | n-type semiconductor.

that increases both regions of oxide with a deficiency and with an excess of aluminium. There remains always a transition layer where there are no electronic charge carriers and the conductivity is very small. This is in accordance with the experiments described in fig. 12. The recovery of the oxide layer after deformation takes place as follows (fig. 13). An electrical tension in the forming direction (aluminium positive) causes a current carried by electrons or holes in the semiconducting layers and by ions in the central layer. The ionic current consists of positive ions going from the *n*-type towards the *p*-type aluminium oxide, or possibly, of negative ions going in the opposite direction. A consequence of this current is that the aluminium surplus and the aluminium deficiency in the semiconducting layers both decrease at the sides of the stoichiometric central layer so that the thickness of the latter increases. If the electric tension is kept constant, the electrical field in the central layer decreases with increasing thickness of this layer. For a certain thickness, the ionic current vanishes almost completely. For a complete recovery of the central layer, a tension considerably less than the forming voltage is sufficient. This appears from the impedance measurements, shown in fig. 13 and from the ballistic measurements given in table VII and fig. 11.

We will make only a few remarks regarding the pre-treatment of the aluminium used, and the applied thermal treatment. Fig. 16a shows the $\rho = \varphi(x)$ curve for an oxide layer formed on aluminium pre-treated by method 2 of section 6. The relatively well conducting part of the layer is thicker than in the case of less well cleaned aluminium. This is an indication that the greater part of the well conducting layer is situated at the metal side. A thermal treatment for some hours at 450 °C causes a great decrease in thickness of the relatively well conducting layers. Perhaps the thermal treatment causes a rearrangement of the oxide lattice, preventing the presence of an excess or deficiency of aluminium in the oxide.

Eindhoven, November 1952

REFERENCES

- 1) W. Ch. van Geel and J. W. A. Scholte, Philips Res. Rep. 6, 54-74, 1951.
- 2) G. Pfoetzer, Z. Naturforschung, 4a, 691-706, 1949.
- 3) F. Rose, Ann. Phys., Lpz., 9, 97-140, 1951.
- 4) F. H. Raymond, Ann. Télécomm. 6, 262-272, 1951.
- 5) W. G. Burgers, A. Claassen and J. Zernike, Z. Phys. 74, 593-603, 1932.
- 6) E. J. W. Verwey, Z. Kristallogr. A 91, 317-320, 1935.
- 7) C. Ervin, Acta cryst. 5, 103-108, 1952.
- 8) W. Hartmann, Z. Phys. 102, 709-733, 1936.
- 9) W. Schottky, Z. Phys. 113, 367-414, 1939; N. F. Mott and R. W. Gurney Electronic processes in ionic crystals, Oxford, University Press, sec. ed., 1948, p. 174.
- 10) W. Ch. van Geel, Physica, 's-Grav., 17, 761-776, 1951.
- 11) B. Davydov, Tech. Phys. U.S.S.R. 5, 87-95, 1938; W. Shockley, Electrons and holes in semiconductors, D. van Nostrand Co., New-York, 1950, Chapter XII.
- 12) W. Ch. van Geel and B. C. Bouma, Philips Res. Rep. 5, 461-475, 1950; 6, 401-424, 1951.
- 13) E. J. W. Verwey, Physica, 's-Grav., 2, 1059-1063, 1935.